Diffusion Problems in Medical Imaging

Shubeur Rahman
Department of Scientific Computing
Simula Research Laboratory,
Martin Linges v 17, Fornebu P.O.Box 134, 1325 Lysaker, Norway

January 15, 2008

Contents

1 Diffuse Optical Tomography

1.1 Introduction

Diffuse optical tomography (DOT) is a potential diagnostic medical imaging technique which utilises the weak absorption of near-infrared (NIR) light by water and both oxygenated (HbO) and deoxygenated hemoglobin (Hb). Biological tissue is illuminated by NIR radiation by an array of sources and the light rays are then reflected, transmitted, or absorbed by the tissue usually after a significant amount of scattering. The scattered light emerging from the tissue is observed by an array of detectors. This data in conjunction with a mathematical model, frequently of a diffusion problem nature, is used to construct spatial maps of absorption and scattering coefficients and hence pathological properties of the material. Current applications of DOT are primarily in the fields of brain function and mammography. The former icludes the examination of a range of cognitive tasks [1, 2] as well as pathological conditions such as changes in HbO and Hb during elliptic siezures [3, 4] and the latter includes the detection of tumours in the breast [5, 6]. The instrumentation is noninvasive, nonionizing, inexpensive, and portable, providing advantages over conventional methods used in medical imaging.

1.2 Photon Diffusion

As a photon propagates through a material with a high optical depth and very short mean free path its behavior becomes dominated by scattering. The path of the photon is effectively a random walk. A large ensemble of such photons can be said to exhibit diffusion in the material, frequently described by a diffusion equation (see Section 1.4.1).

The scattering of the photon generally complicates imaging of tissue structure and function; since transmitted or reflected light re-emerging from the tissue has followed a very complicated path, any localization of absorption or scattering or other optical parameters is lost when we simply observe the light as it exits the tissue. Some of the key processes that occur when a photon is incident on a surface is illustrated in Figure 1. The scattering of the light obscures the image of the underlying structures and complicates the computation of structural and functional unformation.

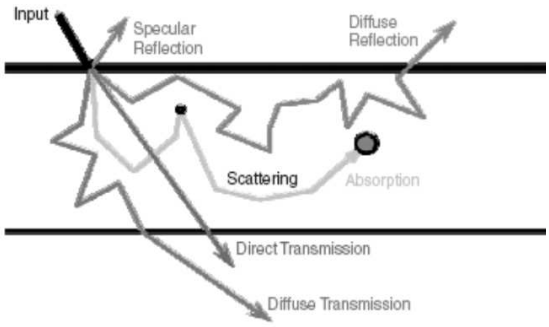

Figure 1: Illustration of scattering, transmission and reflection of a ray of light. Figure taken from [7]

1.3 Near-Infrared Light

The DOT method utilizes the weak aborption of near-infrared radiation by water, HbO and Hb. Figure 2 shows the absorption spectrum of the three absorbers. At smaller wavelengths, the absorption by water increases rapidly and thus complicates DOT imaging. The difference in the absorption coefficient of HbO and Hb allow the resolution of the concentrations of both types of molecules.

The basic idea of DOT imaging is to illuminate the tissue with an array of light sources and to measure the light leaving the tissue with an array of detectors. For each source location, one records an image of the light reaching each detector from that particular source. A model of the propagation of light in tissue is developed and parameterized in terms of the unknown scattering and/or absorption as a function of position in the tissue. Then, using the model together with the ensemble of images over all the sources, one attempts to "invert"' the propagation model to recover the parameters of interest, or, in other words, to estimate the scattering and/or absorption parameters out of the data, using the model.

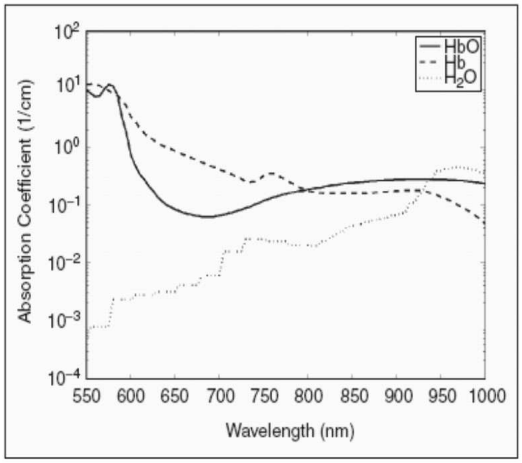

Figure 2: Hemoglobin and water absorption coefficients per mole as a function of wavelength. Note the relatively low absorption between 700 and 1000 nm and the crossover point around 800 nm. Data taken from [8].

1.4 Modeling of Photon Propagation in Highly Scattering Media

To model the propagation of light in highly scattering media, the light is treated as a particle, propagating through a medium of well-defined absorption and scattering characteristics. (In principle Maxwells equations can be solved for complex systems with spatially varying permittivity. However, in practice most models are based on a particle interpretation of light.) The model incorporates interactions only between light particles and the medium and not among light particles themselves. This model also does not take into account polarization effects. Thus a conservation of radiance equation results, known as the radiative transport equation (RTE):

$$\begin{aligned} &\frac{1}{c}\frac{\partial I}{\partial t} + \hat{s}\cdot\nabla I(\mathbf{r},t,\hat{s}) + (\mu_a+\mu_s)I(\mathbf{r},t,\hat{s}) \\ &= \mu_s\int_{4\pi} f(\hat{s},\hat{s}')I(\mathbf{r},t,\hat{s}')d^2\hat{s}' + q(\mathbf{r},t,\hat{s}), \end{aligned} \tag{1}$$

which describes the change of the radiance $I(\mathbf{r},t,\hat{s}')$ at position $\mathbf{r}$ in direction $\hat{s}$. The parameters μ_a and μ_s are the absorption and scattering coefficients

respectively, c is the velocity of light in the medium, and the function $f(\hat{s}, \hat{s})$ is the scattering phase function characterizing the intensity of a wave incident in direction $\hat{s}'$ scattered in direction $\hat{s}$.

The RTE is a balance equation describing the change of energy radiance $I(\mathbf{r}, t, \hat{s}')$ in time due to changes in energy flow: loss due to absorption and scattering, and gain due to scattering and radiation sources. I is defined so that the energy transfer per unit time by photons in a unit solid angle $d^2\hat{s}$ through an elemental area da given by its unit normal $\hat{n}$, at position r, is given by

$$I(\mathbf{r}, t, \hat{s}')\hat{s}' \cdot \hat{n}\, da\, d^2\hat{s}. \tag{2}$$

The diffusion and Monte Carlo schemes discussed in the following sections are derived from the RTE.

1.4.1 Photon Diffusion Equation

A deterministic diffusion model may be derived from the RTE [9, 10, 11]. The approach assumes the reduced scattering coefficient, μ_s', to be small compared to the absorption coefficient.

$$-\nabla \cdot D\nabla\Phi(\mathbf{r}, t) + \nu\mu_a\Phi(\mathbf{r}, t) + \frac{\partial\Phi(\mathbf{r}, t)}{\partial t} = \nu S(\mathbf{r}, t), \tag{3}$$

where $S(\mathbf{r}, t)$ is the equivalent isotropic source and D is the diffusion coefficient, $D = \frac{\nu}{3\mu'}$

Note that near a boundary such as an air-tissue interface, photons which scatter out of the medium will not be scattered back in. Thus here the diffusion approximation does not hold, and so this must be handled as a special boundary condition; a number of models have been proposed and studied, trading off accuracy for computational ease [10, 12].

1.4.2 Solution Methods For The Diffusion Equation

The most frequently applied approaches in the solution of the diffusion equation in the context of DOT are analytic methods based on Green's functions, and numerical procedures based on finite difference methods and finite element methods.

The Green's function approach models the sources in DOT as a δ-function. Green functions have been calculated for various homogenous geometries [13, 14].

The finite difference method has been applied extensively in the forward problem in DOT. The optimal approach for the diffusion equation is the multi-grid method [15, 16] in the frequency domain and alternating direction implicit scheme in the time domain [17].

The finite element method is a more felxible numerical approach than the finite difference method allowing the modelling of devices of more complex geometries. The approach has been applied to both forward [18] and inverse problems [19] in DOT as well as the RTE [20].

1.4.3 Frequency-Domain Photon Diffusion Equation

The Fourier transform of the constant scattering form of Eq. (3) with respect to time results in the frequency-domain photon diffusion equation:

$$[\nabla^2 + k^2]\Phi(\mathbf{r}, \omega) = \frac{-\nu}{D} S(\mathbf{r}, \omega), \tag{4}$$

where k is the complex wavenumber given by

$$k^2 = \frac{-\nu\mu_a + j\omega}{D} = 3\mu_s' \left(-\mu_a + j\frac{\omega}{\nu}\right). \tag{5}$$

The frequency domain systems can employ light sources and detectors which are significantly less expensive than those required for time-resolved systems although time resolved systems have the added capability to acquire information at all frequencies simultaneously.

1.5 Image Reconstruction

The formation of an image representing one or more internal optical characteristics from a series of boundary measurements is an example of a so-called inverse problem. Specifically, it involves the recovery of the parameters of an appropriate model, such as described in Section 1.4.1. The forward problem can be stated as follows:

Given a distribution of light sources $\mathbf{q}$ *on the boundary* $\partial\Omega$ *of an object* Ω*, and a distribution of tissue parameters* $\mathbf{p}$ *within* Ω*, find the resulting measurement set* $\mathbf{y}$ *on* $\partial\Omega$*.*

The solution to the forward problem can be expressed in the form of a general non-linear forward operator:

$\mathbf{y} = F[\mathbf{p}]$.

Similarly, the inverse problem may be stated as follows:

Given a distribution of light sources $\mathbf{p}$ *and a distribution of measurements* $\mathbf{y}$ *on* $\partial\Omega$ *derive the tissue parameter distribution* $\mathbf{p}$ *within* Ω

and this can be represented by

$\mathbf{p} = F^{-1}[\mathbf{y}]$.

1.5.1 Recent Work on DOT Inverse Solutions

DOT is a nonlinear, ill-posed, and generally underdetermined imaging problem. This results in difficulties in finding a unique solution to the inverse problem. Some of the mathematical tools applied in the solution process include regularization, optimization, statistical modeling, and parametric representations. Regularization techniques are used to stabilize inversion of forward models against ill-conditioning caused by the ill-posedness of the inverse problem [21, 22, 23]. In brief, regularization consists of adding a second term to be minimized in defining a good solution to a standard least-squares fit of the estimate to the data; for example, if we are only interested in imaging the absorption coefficient μ_a, using fluence measurements y and forward model $h(\mu_a)$, we solve

$$\hat{\mu}_a = argmin_{\mu_a}||y - h(\mu_a)||_2^2 + \lambda^2 R(\mu_s), \tag{6}$$

where the first term enforces the fit of the solution to the measured fluence, the second enforces a constraint based on an a priori assumption about how a reasonable solution should behave, and is called the regularization parameter and governs the tradeoff between the two terms. Typically R is a norm or the norm of a derivative so as to penalize solutions that are too large or too rough. Choosing the value of is often critical and sensitive, and there is a vast literature on this topic (see [21], for instance, for a discussion).

2 Positron Emmission Tomography

Positron emission tomography (PET) is a nuclear medicine medical imaging technique which produces a three-dimensional image or map of functional processes in the body. The technique was first developed by Michel (Michael) Ter-Pogossian, Michael E. Phelps and others at the Washington University School of Medicine in 1975 [1][2]

To conduct the scan, a short-lived radioactive tracer isotope, which decays by emitting a positron, which also has been chemically incorporated into a metabolically active molecule, is injected into the living subject (usually into blood circulation). There is a waiting period while the metabolically active molecule becomes concentrated in tissues of interest; then the research subject or patient is placed in the imaging scanner. The molecule most commonly used for this purpose is fluorodeoxyglucose (FDG), a sugar, for which the waiting period is typically an hour.

As the radioisotope undergoes positron emission decay (also known as positive beta decay), it emits a positron, the antimatter counterpart of an electron. After travelling up to a few millimeters the positron encounters and annihilates with an electron, producing a pair of annihilation (gamma) photons moving in almost opposite directions. These are detected when they reach a scintillator material in the scanning device, creating a burst of light which is detected by photomultiplier tubes or silicon avalanche photodiodes (Si APD). The technique depends on simultaneous or coincident detection of the pair of photons; photons which do not arrive in pairs (i.e., within a few nanoseconds) are ignored.

The most significant fraction of electron-positron decays result in two 511 keV gamma photons being emitted at almost 180 degrees to each other; hence it is possible to localize their source along a straight line of coincidence (also called formally the "line of response" or LOR). In practice the LOR has a finite width as the emitted photons are not exactly 180 degrees apart. If the recovery time of detectors is in the picosecond range rather than the 10's of nanosecond range, it is possible to calculate the single point on the LOR at which an annihilation event originated, by measuring the "time of flight" of the two photons. This technology is not yet common, but it is available on some new systems [1]. More commonly, a technique much like the reconstruction of computed tomography (CT) and single photon emission computed tomography (SPECT) data is used, although the data set collected in PET is much poorer than CT, so reconstruction techniques are

more difficult (see section below on image reconstruction of PET). Using statistics collected from tens-of-thousands of coincidence events, a set of simultaneous equations for the total activity of each parcel of tissue along many LORs can be solved by a number of techniques, and thus a map of radioactivities as a function of location for parcels or bits of tissue "voxels"), may be constructed and plotted. The resulting map shows the tissues in which the molecular probe has become concentrated, and can be interpreted by a nuclear medicine physician or radiologist in the context of the patient's diagnosis and treatment plan.

PET is both a medical and research tool. It is used heavily in clinical oncology (medical imaging of tumors and the search for metastases), and for clinical diagnosis of certain diffuse brain diseases such as those causing various types of dementias. PET is also an important research tool to map normal human brain and heart function.

PET is also used in pre-clinical studies using animals, where it allows repeated investigations into the same subjects. This is particularly valuable in cancer research, as it results in an increase in the statistical quality of the data (subjects can act as their own control) and substantially reduces the numbers of animals required for a given study.

Radionuclides used in PET scanning are typically isotopes with short half lives such as carbon-11 (20 min), nitrogen-13 (10 min), oxygen-15 (2 min), and fluorine-18 (110 min). Due to their short half lives, the radionuclides must be produced in a cyclotron which is not too far away in delivery-time to the PET scanner. These radionuclides are incorporated into compounds normally used by the body such as glucose, water or ammonia and then injected into the body to trace where they become distributed. Such labelled compounds are known as radiotracers.

The raw data collected by a PET scanner are a list of 'coincidence events' representing near-simultaneous detection of annihilation photons by a pair of detectors. Each coincidence event represents a line in space connecting the two detectors along which the positron emission occurred.

Coincidence events can be grouped into projections images, called sinograms. The sinograms are sorted by the angle of each view and tilt, the latter in 3D case images. The sinogram images are analogous to the projections captured by computed tomography (CT) scanners, and can be reconstructed in a similar way. However, the statistics of the data is much worse than those obtained through transmission tomography. A normal PET data set has millions of counts for the whole acquisition, while the CT can reach a

few billion counts. Furthermore, PET data suffer from scatter and random events much more dramatically than CT data does.

In practice, considerable pre-processing of the data is required - correction for random coincidences, estimation and subtraction of scattered photons, detector dead-time correction (after the detection of a photon, the detector must "cool down" again) and detector-sensitivity correction (for both inherent detector sensitivity and changes in sensitivity due to angle of incidence).

Filtered back projection (FBP) has been frequently used to reconstruct images from the projections. This algorithm has the advantage of being simple while having a low requirement for computing resources. However, shot noise in the raw data is prominent in the reconstructed images and areas of high tracer uptake tend to form streaks across the image.

Iterative expectation-maximization algorithms are now the preferred method of reconstruction. The advantage is a better noise profile and resistance to the streak artifacts common with FBP, but the disadvantage is higher computer resource requirements.

2.1 SAFE: The Oslo Cyclotron Laboratory

The Oslo Cyclotron Laboratory (OCL) was built in 1979, and has been the basis of Norwegian experimental nuclear physics the last twenty years. The MC-35 Scanditronix cyclotron is the only accelerator in Norway for ionized atoms and are used today in various fields of research and applications. The main topic of nuclear physics at OCL is the investigation of level densities and radiative strength functions. These quantities are important for the understanding of thermodynamic and electromagnetic properties of the atomic nucleus. Also these studies are essential for the understanding of stellar evolution, as well as accelerator-driven transmutation of nuclear waste.

In parallel with basic nuclear physics and chemistry research, the cyclotron is used for the production of radioactive isotopes. Several groups have taken advantage of this instrument in the field of nuclear medicine. Today it is an exponential growth in the use of radioactive isotopes in medicine. The main user is the Norwegian Radium Hospital in Oslo, where radioactive 18F is produced for positron emission tomography (PET). The cyclotron can also produce 211At, 205Bi and certain other isotopes for future cancer therapy.

2.2 Applications of Monte Carlo methods in medical imaging

Detector modelling. Many detector modeling applications were developed in the PET field, including the pioneering work of Derenzo [**?**] who simulated arrays of detectors of different materials and sizes to study the effect of the inter-crystal septa and later on to optimize the optical coupling between BGO crystals and PMTs88 by taking into account the reflection and scattering along the detection system.

Imaging systems and collimators design. Image modeling was employed by Schulz [**?**] who devised a computer program simulating a rectilinear scanner which was used to study the influence of different imaging protocols on the detectability of lesions. Simulation of gamma camera imaging to assess qualitatively and quantitatively the image formation process and interpretation103 and to assist development of collimators104 using deterministic methods and simplifying approximations have been developed mainly to improve speed of operation.

Image reconstruction algorithms. Monte Carlo simulations have been shown to be very useful for validation and comparative evaluation of image reconstruction techniques since it is possible to obtain a reference image to which reconstructed images should be compared. Three different algorithms for performing PET image reconstruction have been compared using Monte Carlo phantom simulations [].

Dosimetry and treatment planning. There is no doubt that the area where early Monte Carlo calculations in the field have been performed is dosimetry modeling and computations [].

References

[1] K. Takahashi et al. Activation of the visual cortex imaged by 24-channel near-infrared spectroscopy. *J. Biomed. Opt.*, 5:93–96, 2000.

[2] H. Koizumi, T. Yamamoto, A. Maki, Y. Yamashita, H. Sato, H. Kawaguchi, and N. Ichikawa. Optical topography: practical problems and new applications. *Appl. Opt.*, 42:305462, 2003.

[3] E. Watanabe, A. Maki, F. Kawaguchi, K. Takashiro, Y. Yamashita, H. Koizumi, and Y. Mayanagi. Non-invasive assessment of language

dominance with near-infrared spectroscopic mapping. *Neurosci. Lett.*, 256:49–52, 1998.

[4] E. Watanabe, Y. Nagahori, and Y. Mayanagi. Focus diagnosis of epilepsy using near-infrared spectroscopy. *Epilepsia*, 43:50–55, 2002.

[5] V. Ntziachristos and B. Chance. Probing physiology and molecular function using optical imaging: applications to breast cancer. *Breast Cancer Res.*, 3:41–6, 2001.

[6] A. Li. Tomographic optical breast imaging guided by three-dimensional mammography. *Appl. Opt.*, 42:5181–5190, 2003.

[7] D. A. Boas, D. H. Brooks, E. L. Miller, C. A. DiMarzio, M. Kilma, R. J. Gaudette, and Q. Zhang. Imaging the body with diffuse optical tomography. *IEEE Signal Processing Magazine*, November:57–75, 2001.

[8] S. A. Prahl. Optical absorption of hemoglobin. *Oregon Medical Laser Center, OR, Tech. Rep.*, 1999.

[9] D. A. Boas. *Diffuse photon probes of structural and dynamical properties of turbid media: Theory and biomedical applications*. PhD thesis, Dept. Physics, Univ. Pennsylvania, Philadelphia, PA, 1996.

[10] R. C. Haskell, T.-T. Tsay L. O. Svaasand, T.-C. Feng, M. S. McAdams, and B. J. Tromberg. Boundary conditions for the diffusion equation in radiative transfer. *J. Opt. Soc. Amer. A*, 11:2727–2741, 1994.

[11] S. R. Arridge. Optical tomography in medical imaging. *Inverse Problems*, 15:R41–R93, 1999.

[12] B. W. Pogue and M. S. Patterson. Frequency-domain optical absoprtion spectroscopy of finite tissue volumes using diffusion theory. *Phys. Med. Biol.*, 39:1157–1180, 1994.

[13] M. S. Patterson, B. Chance, and B. C. Wilson. Time resolved reflectance and transmittance for the non-invasive measurement of tissue optical properties. *Appl. Opt.*, 28:23312336, 1989.

[14] G. Eason, A. Veitch, R. Nisbet, and F. Turnbull. The theory of the backscattering of light by blood. *J. Phys. D: Appl. Phys.*, 1:14631479, 1978.

[15] W. Hackbush. *Multigrid Methods and Applications.* Berlin: Springer, 1980.

[16] B. W. Pogue, M. S. Patterson, H. Jiang, and K. D. Paulsen. Initial assessment of a simple system for frequency domain diffuse optical tomography. *Phys. Med. Biol.*, 40:17091729, 1995.

[17] W. F. Ames. *Numerical Methods for Partial Differential Equations.* New York: Academic, 1977.

[18] S. R. Arridge, M. Schweiger, M. Hiraoka, and D. T. Delpy. A finite element approach to modelling photon transport in tissue. *Med. Phys.*, 20:299309, 1993.

[19] M. Schweiger, S. R. Arridge, M. Hiraoka, M. Firbank, and D. T. Delpy. Initial assessment of a simple system for frequency domain diffuse optical tomography. *Comparison of a finite element forward model with experimental phantom results: application to image reconstruction Proc. SPIE 1888*, page 179190, 1993.

[20] C. R. E. de Oliveira. An arbitrary geometry finite element method for multigroup neutron transport with anisotropic scattering. *Prog. Nucl. Energy*, 18:227236, 1986.

[21] P. C. Hansen. *Rank-Deficient and Discrete Ill-Posed Problems.* Philadelphia, PA: SIAM, 1998.

[22] A. Tikhonov and V. Arsenin. *Solution of Ill-Posed Problems.* Washington, DC: Winston, 1977.

[23] C. W. Groetsch. *The Theory of Tikhonov Regularization for Fredholm Equations of the First Kind.* Boston, MA: Pitman, 1984.